

30 characterizing the engineering performance of warm CRMA prepared by six different mixing
31 sequences. Properties including Marshall stability and flow value, workability, rheological
32 property, rutting resistance, moisture sensitivity and fatigue resistance of prepared mixtures were
33 measured and compared. Analytic hierarchy process (AHP) was employed to determine the optimal
34 mixing sequence of warm CRMA considering the overall engineering performance. Test results
35 showed that the effect of warm CRMA's mixing procedure on its engineering performance is
36 noticeable. Earlier incorporation of surfactant additive had limited negative influence on
37 mechanical properties of warm CRMA but allows for more energy saving during the production of
38 rubberized asphalt binder. The AHP analysis results indicated that among the six mixing sequences,
39 the optimal option is to make rubber absorb surfactant first, then incorporating the rubber-surfactant
40 compound to raw asphalt and finally blending the modified binder to aggregates.

41 **KEYWORDS:** Crumb rubber modified asphalt mixture; Warm mix asphalt; Mixing procedure;
42 Engineering performance

43 1. INTRODUCTION

44 Asphalt mixture has been extensively used for pavement construction owing to merits including
45 improved smoothness, low traffic noise, easy maintenance and rapid construction (Leng et al., 2018;
46 Zaumanis et al., 2018; Xu et al., 2019). The wide application of asphalt materials provides a
47 potential approach to recycle industrial and domestic wastes, including plastic (Ahmadinia et al.,
48 2011), waste packing tape (Yu et al., 2019a), seashells (Ruiz et al., 2018), cigarette butts
49 (Mohajerani et al., 2017), reclaimed asphalt pavement (Zhao et al., 2012; Zhao et al., 2013; Song
50 et al., 2018) and rubber tires (Liu et al., 2012). On one hand, the consumption of above refuse is an
51 efficient way of waste management; on the other hand, the components within waste materials
52 bring certain enhancement on performance of asphalt materials. Especially, the feasibility of using

53 crumb rubber modifier (CRM) derived from waste vehicular tires as asphalt modifier has been
54 demonstrated by both laboratory investigations and field surveys. (Moreno et al., 2013; Jia et al.,
55 2015; Bai et al, 2016; Gong et al., 2018; Yu et al., 2018; Ling et al., 2019). In recent decades, many
56 studies have been conducted to characterize the effect of CRM on the performance related
57 properties of asphalt materials. These studies reported the superior service performance of CRMA
58 in comparison with unmodified asphalt mixture and some other polymer modified asphalt mixtures.
59 For example, based on both laboratory and field evaluation, Huang et al. reported that CRMA
60 showed overall satisfied service performance including rutting, fatigue, and pavement roughness
61 (Huang et al., 2002). A Brazilian study proven that the use of asphalt rubber (AR) binder
62 significantly improved the rutting resistance of asphalt mixture (Fontes et al., 2010). Ding et al.
63 (2017) found that the service performance, including rutting resistance, cracking resistance,
64 moisture stability, and fatigue failure resistance, of CRMA is comparable to that of styrene–
65 butadiene-styrene (SBS) modified asphalt mixture. In addition to the above-mentioned mechanical
66 properties, addition of crumb rubber was also found to be able to reduce the noise generated by
67 tire/pavement interaction (Vázquez et al., 2016) and to improve the anti-icing performance of
68 asphalt pavement (Wei et al., 2016).

69 As known, two mixing process are available to prepare CRMA, namely, dry process and wet
70 process (Chávez et al., 2019). In dry process, approximately 1% to 3% by weight of aggregate is
71 substituted by crumb rubber. In wet process, crumb rubber works as a binder modifier. CRM is
72 incorporated into raw asphalt as modifier and then the modified binder is blended to aggregates to
73 prepare CRMA. By comparison, CRMA prepared by wet process exhibited superior engineering
74 performance than that with dry process, as both the polymer modification and resilient particle
75 effect of CRM are fully utilized (Ranieri et al., 2017; Chávez et al., 2019). However, it is worth
76 noting that the incorporation of CRM significantly increases the viscosity of asphalt binder,

77 resulting in higher mixing and paving temperature. Hence, the application of CRMA mixtures,
78 especially those with wet process, carries environmental concerns and increases the energy
79 consumption during its producing and paving process (Xiao et al., 2012). One effective approach
80 to address the workability concern of CRMA is to incorporate warm mix asphalt (WMA)
81 technology (Wei et al., 2016). Based on the working mechanism, WMA technologies can be
82 grouped into three categories: foaming technologies, addition of organic additives, and addition of
83 chemical additives (Rubio et al., 2012). WMA additives are able to enhance the workability of
84 CRMA, but their influence on other properties varies (Xiao et al., 2010; Wang et al., 2012; Yu et
85 al., 2018; Yu et al., 2019b). For instance, chemical WMA additives are liquid surfactants which
86 reduce the friction between asphalt binder and aggregate during their blending process. It is reported
87 that surfactant can decrease the production temperature of CRMA by 15-30 °C without obviously
88 deteriorating the mechanical properties (Paje et al., 2010; Cao and Liu, 2012; Oliveira et al., 2013;
89 Yu et al., 2017).

90 Most of available studies on warm CRMA (WCRMA) focused on the effect of WMA type
91 and dosage on binder and mixture properties. However, the mixing sequence of different
92 components, which may exert significant difference on performance, has been ignored. For the
93 preparation of WCRMA, apart from the conventional dry and wet process, the addition of WMA
94 additive provides extra options of mixing sequences. Previous research reported that mixing
95 sequence of warm mix asphalt affects the properties of warm AR binder (Paje et al., 2010; Yu et
96 al., 2017). It was also proven that the early addition of surfactant additive had very marginal
97 negative effect on rheological properties of AR binder (Yu et al., 2017). Nevertheless, limited
98 studies focusing on optimizing the mixing sequence of WCRMA mixtures can be found.

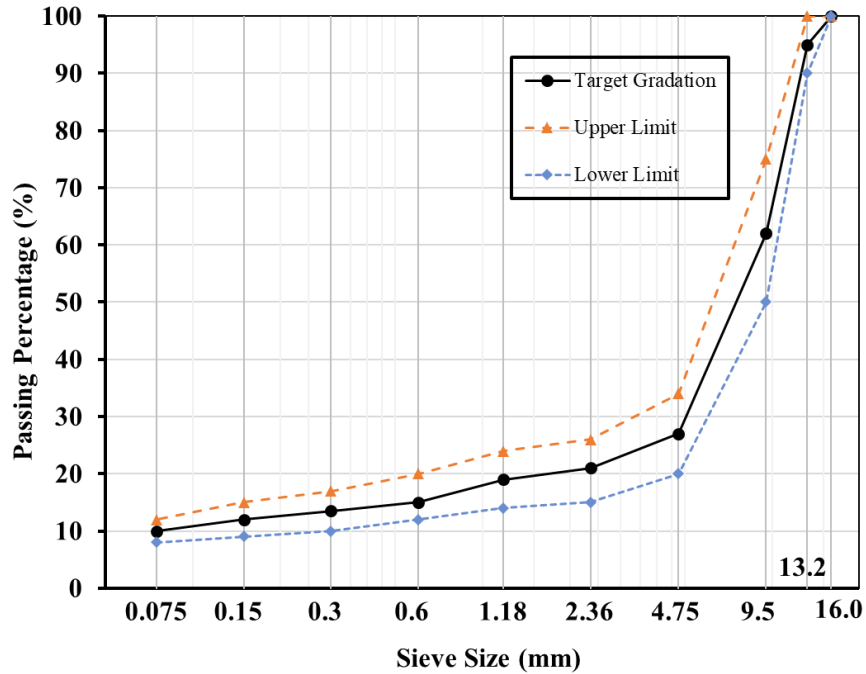
99 To this end, this study aims to optimize the mixing sequences of CRMA mixtures with liquid
100 surfactant additive. It is a follow-up study of the previous paper about mixing procedure of warm
101 AR binder (Yu et al., 2017). In this paper, hot and warm CRMA mixtures were prepared with
102 conventional dry/wet process and other four potential mixing sequences. The workability and
103 service performance related properties including Marshall stability, stiffness modulus, moisture
104 damage resistance, rutting resistance, and fatigue failure resistance of the prepared CRMAs and
105 control asphalt mixture (unmodified asphalt mixture) were then compared to study the influence of
106 mixing sequence. Analytic Hierarchy Process (AHP) was employed to determine the priority of
107 mixing procedure considering the overall engineering performance of asphalt mixtures. It is
108 believed that by means of optimizing the mixing procedure of CRMA, it might be able to prepare
109 CRMA with optimal engineering performance and minimum energy consumption.

110 **2. EXPERIMENTAL PROGRAM**

111 **2.1. Raw materials**

112 The engineering properties of raw asphalt with a penetration grade of 60-80 (0.1 mm), which is
113 chosen as the base binder in this study, are shown in Table 1.

114 Aggregate used in this study was basalt, provided by Central Fortune Creation (Canton)
115 Roadway Technology Co., Ltd. Diabase filler, which is commonly used in southern China, was
116 selected as mineral filler. SMA13 mixture with 4% designed air void was chosen to prepare hot
117 and warm CRMA. The gradation of the aggregate is shown in Figure 1.



118

119

Figure 1. Aggregate Gradation

120 Physical properties of Evotherm-DAT can be found in previous studies (Yu et al., 2017; Yu
 121 et al., 2018). The dosage of the Evotherm-DAT was set as 5% by weight of asphalt binder according
 122 to the manufacture’s recommendation. 40 mesh crumb rubber was used, and the dosage was 18%
 123 by weight of virgin binder. The gradation of crumb rubber is shown in Table 2.

124

Table 1. Engineering properties of virgin binder

Properties	Unit	Pen60/70 binder	Specification
Penetration	0.1mm	64.5	ASTM D5
Softening point	°C	48.9	ASTM D36
Solubility	%	99.9	AASHTO T 44-13
Separation difference	°C	0.2	BS EN 12697-15
Critical temperature when $G^*/\sin\delta=1.0$ kPa	°C	68.7	AASHTO TP 101

Rotational viscosity (135 °C/160 °C)	cp	480/170	AASHTO T316
After short-term aging			
Mass loss	%	-0.08	ASTM D2872
Critical temperature when $G^*/\sin\delta=2.2$ kPa	°C	66	AASHTO TP 101
After long-term aging			
Critical temperature when $G^*\sin\delta=5$ MPa	°C	22.5	AASHTO TP 101
Low-temp stiffness (- 6/-12 °C)	MPa	121/222	AASHTO T313
m-value (-6/-12 °C)	-	0.386/0.316	AASHTO T313

125

Table 2. Gradation of crumb rubber

BS sieve size	Passing rate
0.6mm	100%
0.425mm	92.3%
0.3mm	58.7%
0.15mm	26.2%
0.075mm	12.5%

126 **2.2. Asphalt mixture**

127 Marshall mix design method was applied to design the asphalt mixture. The optimal asphalt binder
 128 content was determined as 6.7%. The volumetric properties of designed mixture can be found in a
 129 previous publication (Yu et al., 2019b).

130 As shown in Table 3, four mixing processes (Process A to Process D) were employed in this
 131 study to prepare WCRMA. In addition, dry- and wet- process were used to prepare hot mix CRMA.
 132 Control asphalt mixture was prepared with conventional hot mixing process, namely, blending
 133 virgin binder and aggregate at 160 °C. In this study, to focus on the effect of mixing sequence, each
 134 type of rubberized asphalt mixture used crumb rubber with same gradation and dosage.

135

Table 3. Involved mixing processes

Mixing Process	Description	Mixture Label
Conventional hot mixing process	Virgin binder was mixed with aggregate at 160 °C	Ctrl
Wet process	CR was added to virgin binder at 176 °C followed by high-speed shearing 60 minutes to prepare AR. The reaction time of 60 minutes was considered as suitable based on the preliminary studies (Yu et al., 2017). AR was then blended with aggregate at 176 °C, same production temperature of AR binder.	WM
Dry process	CR, aggregate and virgin binder were directly mixed at 160 °C to prepare asphalt mixture.	DM
A	The prepared AR, aggregates, and Evotherm-DAT were mixed together at 160 °C.	W-EM
B	CR, virgin binder and Evotherm-DAT were mixed directly using a high-speed shear mixer at 160 °C for 60 minutes to prepare ARE. Asphalt mixture was prepared by mixing the prepared ARE with aggregates at 160 °C.	AREM
C	Evotherm DAT were absorbed by CR by immersing CR in the Evotherm DAT for 24 hours (Yu et al., 2017). CR which absorbed Evotherm-DAT were blended to virgin binder at 160 °C for 60	REM

	minutes to prepare modified asphalt binder (ER-A). ER-A was added to aggregate at 160 °C to prepare asphalt mixture.	
D	CR, Evotherm-DAT, aggregate and asphalt binder were directly mixed together at 160 °C.	D-EM

136 **2.3. Sample Preparation**

137 In this study, four compaction methods, namely, Superpave gyratory compactor (SGC), standard
138 Marshall method, and two types of segmented rolling compactors were employed to prepare test
139 specimens. Based on experience obtained in previous studies, the blending temperature of WM
140 was set at 176 °C, while that of other asphalt mixtures was set as 160 °C (Yu et al., 2018; Yu et al.,
141 2019b). Cylindrical samples with the dimension of 150 mm in diameter and 95 ± 5 mm in height
142 were compacted by SGC for moisture damage resistance test (AASHTO R 83, 2017). Superpave
143 simple performance test was performed on test specimens (150 mm in height and 100 mm in
144 diameter) cored from SGC-compacted samples. Cylindrical samples with the dimension of 101.5
145 mm in diameter and 63.5 mm in height for Marshall stability and flow value test were compacted
146 using standard Marshall method. 300 mm × 300 mm × 50 mm asphalt mixture slabs were prepared
147 using segmented rolling compactor for rutting test. Beam-shape specimens (380 mm × 50 mm ×
148 63 mm) were extracted from the compacted slab (450 mm × 150 mm × 185 mm) for four-point
149 bending fatigue test.

150 **3. TESTING PROGRAM**

151 **3.1. Marshall stability and flow value tests**

152 The conventional Marshall stability and flow values of all the asphalt mixture were obtained in
153 accordance with ASTM D6927 (2015). Marshall stability refers to the maximum force the samples

154 can withstand at the standard loading condition (a constant loading speed of 50mm/min). The
155 amount of deformation of the samples when loaded to failure is expressed as the flow value. For
156 each type of asphalt mixture, three replicate tests were performed.

157 **3.2. Workability test**

158 Since there is no standard test method for evaluating the workability of asphalt mixture, load cycles
159 of Superpave gyratory compactor (SGC) was employed in this study to investigate the workability
160 of asphalt mixtures prepared with various mixing procedures according to previous papers (Yu et
161 al., 2018; Yu et al., 2019a). Loose asphalt mixture with same weight was compacted using SGC. 4
162 cm was set as the target height of compacted asphalt mixture and the corresponding load cycles
163 were collected to reveal the workability of asphalt mixture (Yu et al., 2019a). Fewer cycles indicate
164 a better workability of asphalt mixture. Three replicate tests were conducted in the workability test.

165 **3.3. Superpave simple performance test**

166 Simple performance test (SPT) was performed to characterize the dynamic modulus of asphalt
167 mixtures according to AASHTO T342 (2011). The tests were performed at five temperatures: -10
168 °C, -4.4 °C, 21.1 °C, 37.8 °C, and 54.4 °C. At each temperature, the tests were performed at the
169 following frequencies: 0.1 Hz, 0.5 Hz, 1 Hz, 5 Hz, 10 Hz, and 25 Hz. The testing temperatures and
170 frequencies were set according to the test standard AASHTO T342 (2011). The dynamic modulus,
171 E^* , was utilized to evaluate the rheological properties of asphalt mixture.

172 **3.4. Moisture damage resistance test**

173 The moisture damage resistance of asphalt mixture was determined by analyzing the indirect tensile
174 strength (ITS) of asphalt mixture before and after freeze-thaw conditioning (ASTM D6931, 2017).

175 The conditioning program includes three phases. The prepared cylindrical specimens were first
176 soaked into water at room temperature followed by placing into vacuum chamber until it achieves
177 at vacuum saturation. The vacuum saturated specimens were then subjected to a freeze-thaw cycle
178 including a -18 °C, 6h freezing process and a 60 °C, 24h thawing process. The specimens were
179 placed into a 25 °C water bath for 2 hours before testing. The ITS of specimen before and after
180 water conditioning was measured. The ITS ratio (ITSR), which is the ratio of specimen's ITS
181 before and after water conditioning, was used to evaluate the moisture damage resistance of asphalt
182 mixtures.

183 **3.5. Rutting test**

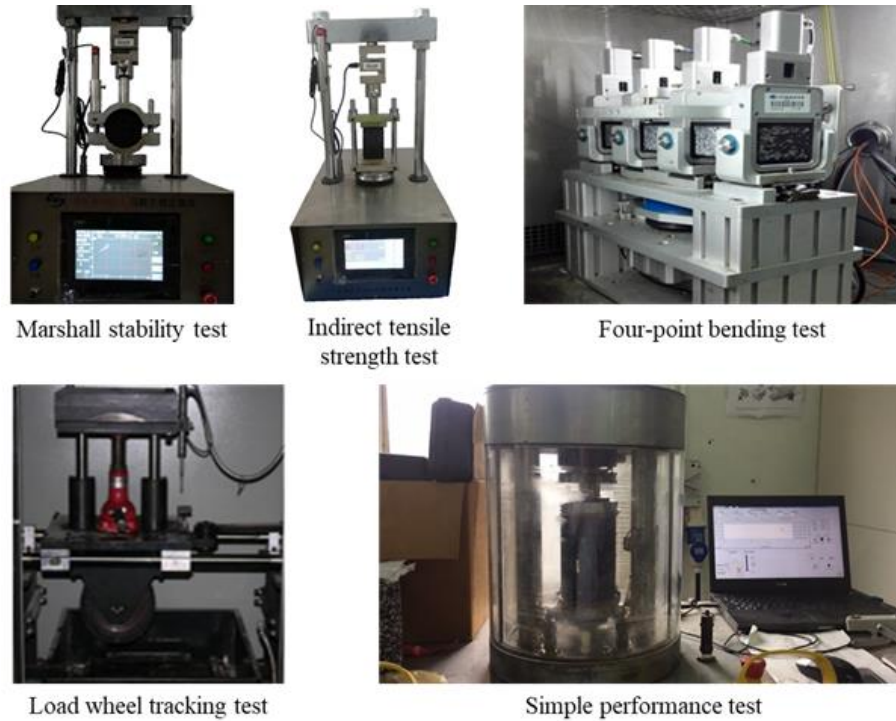
184 The rutting resistance performance of asphalt mixtures were investigated using loading wheel-
185 tracking (LWT) test (ASTM D6372, 2015). The LWT test was performed at 60 °C which is
186 regarded as the maximum service temperature of asphalt pavement. The wheel-tracking rate and
187 rut depth were measured by applying a load to the single rubber wheel under 520 N for 45 minutes.
188 Two parameters were used for rutting resistance characterization, i.e., rutting depth (the measured
189 deformation of sample surface relative to the original surface) and rutting rate (the rate of rutting
190 development at the final 15 minutes).

191 **3.6. Fatigue test**

192 The fatigue response of asphalt mixture under repeated load were characterized using four-point
193 bending (4PB) test (ASTM D7460, 2010). All the 4PB tests were performed at 15 °C. The fatigue
194 life of the tested specimen was defined as the number of loading cycles when the modulus of the
195 specimen attenuated by 50% of its initial modulus. The initial modulus was measured at 50th

196 loading cycle. Four microstrain levels, i.e., 400, 600, 800, and 1000, were selected to evaluate the
197 fatigue response of asphalt mixture specimens.

198 Figure 2 presents the laboratory tests conducted in this study.



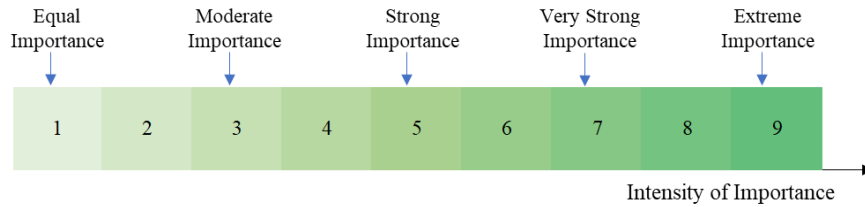
199

200 **Figure 2. Experimental tests conducted in this study**

201 **3.7. Analytic Hierarchy Process (AHP)**

202 The analytic hierarchy process (AHP) was developed by Thomas L. Saaty for organizing and
203 analyzing complex decisions based on mathematic and psychology (Satty, 1990). AHP is a multi-
204 criteria decision making approach, it ranges the factors affecting goal in a hierarchic structure
205 descending from overall goal to criteria, sub-criteria and alternative in successive levels. In
206 comparison with traditional decision tree, AHP is able to represent a different cut at the problem at
207 each level. The procedure of using AHP decision process can be mainly separated into three steps:
208 structure the problem as a hierarchy, evaluate the hierarchy, and establish priorities. The final

209 decision is made based on the established priorities. The first step aims to provide an overall view
 210 with respect to the complex relationships inherent in the situation. At second step, the hierarchy is
 211 evaluated by means of pairwise comparison. Every goal, criterions, and alternatives are termed as
 212 nodes. Pairwise comparisons were performed on the nodes at each level. Specifically, the nodes at
 213 same level were compared, two by two, with respect to their contribution to the nodes above them.
 214 The pairwise comparison result, a_{ij} , represents the relative importance of node i to j and is given a
 215 corresponding intensity of importance. In AHP, there are mainly five scales of intensity of
 216 importance, namely, 1, 3, 5, 7, 9. From 1 to 9, the intensity of importance gradually increases. The
 217 intensities of 2, 4, 6, 8 were used to express intermediate values. The main scales for pairwise
 218 comparisons were listed in Figure 3.



219
 220 **Figure 3. Main scales for pairwise comparison**

221 If there are n alternatives, A_1, \dots, A_n , whose weights are $\omega_1, \dots, \omega_n$, respectively, then the
 222 pairwise comparison matrix, A , is desired to satisfy the following equation:

$$\begin{matrix} & A_1 & A_2 & \dots & A_n \\ A_1 & \begin{bmatrix} a_{1,1} & a_{1,2} & \dots & a_{1,n} \end{bmatrix} \\ A_2 & \begin{bmatrix} a_{2,1} & a_{2,2} & \dots & a_{2,n} \end{bmatrix} \\ \vdots & \begin{bmatrix} \vdots & \vdots & & \vdots \end{bmatrix} \\ A_n & \begin{bmatrix} a_{n,1} & a_{n,2} & \dots & a_{n,n} \end{bmatrix} \end{matrix} \begin{bmatrix} \omega_1 \\ \omega_2 \\ \vdots \\ \omega_n \end{bmatrix} = n \begin{bmatrix} \omega_1 \\ \omega_2 \\ \vdots \\ \omega_n \end{bmatrix} \quad \text{Equation 1}$$

223 Where, $a_{ij} = \omega_i/\omega_j$, n is the size of matrix A . Mathematically, n is the eigenvalue of A , and
 224 ω is the associated eigenvector.

225 Given this, by solving equation, $AX = \lambda X$, the weights of alternatives can be obtained.
226 Assume λ_{\max} is the principal eigenvalue of A , X_{\max} is the corresponding eigenvector, namely weight
227 vector of the alternatives, then λ_{\max} should satisfy Equation 2.

$$C.R. = \frac{C.I.}{R.I.} = \frac{\lambda_{\max} - n}{n - 1} < 0.1 \quad \text{Equation 2}$$

228 where,

229 C.R. is consistency ratio,

230 C.I. is consistency index,

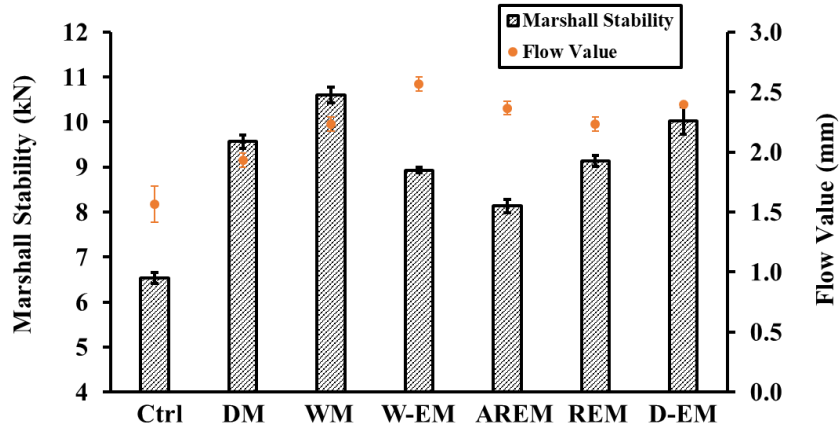
231 R.I. is random consistency index.

232 n is size of matrix.

233 4. RESULTS AND DISCUSSION

234 4.1. Marshall stability and flow value

235 Figure 4 presents the Marshall stabilities and flow values of asphalt mixtures. Marshall stability is
236 an indicator of mixture performance at high temperature. Flow value relates to the stiffness of
237 asphalt mixture. Asphalt mixture with a lower flow value is less susceptible to permanent
238 deformation at high service temperature but more sensitive to low temperature thermal cracking.
239 Both Marshall stability and flow value are involved in the Marshall design method as fundamental
240 indicators.



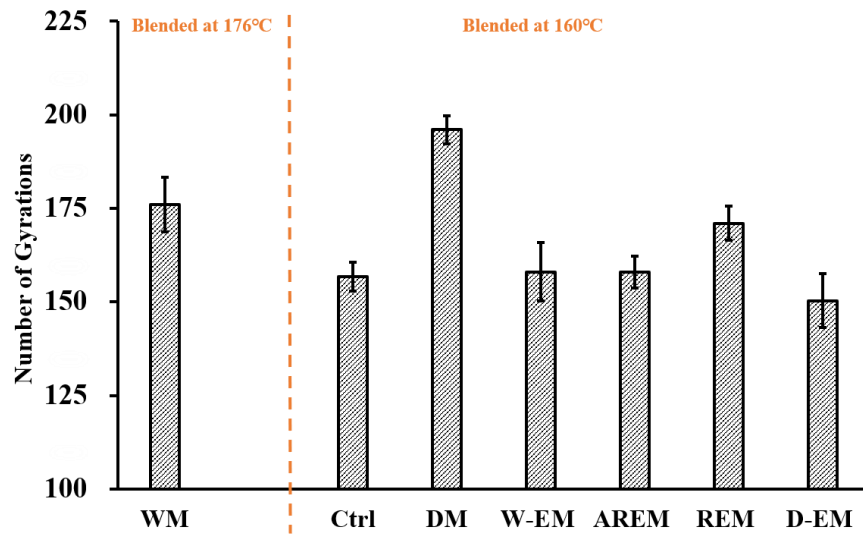
241
242 **Figure 4. Marshall stability and flow values of asphalt mixtures**

243 As can be seen in Figure 4, all CRMAs had higher Marshall stabilities than Ctrl, this is benefit
 244 from the addition of CRM. Among the CRMAs, Marshall stability changes varied along the
 245 different mixing sequences. WM exhibited the best high-temperature performance followed by DM,
 246 while that of AREM was the poorest. For WCRMAs, D-EM and AREM had the highest and lowest
 247 Marshall stability, respectively. Similarly, flow value was also affected by the mixing procedure.
 248 Among WCRMAs, W-EM presented the highest flow value, while that of REM was the lowest.

249 **4.2. Workability**

250 Workability refers to the difficulty of mixing and compacting asphalt mixture, the better the
 251 workability, the easier the mixing and compaction. Workability has been regarded as one of the
 252 critical indicators for asphalt mixture as it is related to the volumetric properties of asphalt mixture
 253 which affects the service performance of asphalt mixture. As abovementioned, the required
 254 compacting cycles of SGC were employed in this study to evaluate the compactibilities of asphalt
 255 mixtures. More gyration numbers indicate more compaction energy and thus poorer
 256 compactibility. Figure 5 presents the required compacting cycles of different asphalt mixtures. As
 257 expected, because of the anti-compacting property of rubber particles in DM, it exhibited the
 258 highest gyrations number indicating the worst workability. The required compacting cycles of

259 CRMA with Evotherm DAT were obviously less than those without Evotherm DAT and similar to
 260 that of Ctrl. It verified the effectiveness of Evotherm DAT with respect to workability improvement
 261 of CRMA regardless of mixing sequence. However, the effect of mixing process on the workability
 262 cannot be ignored. REM and D-EM required the maximum and minimum load cycles, respectively
 263 with a difference of 13 cycles. While, the gyration numbers of three other WCRMAs were quite
 264 close together at around 158. Based on the results of required compacting cycles, the workability
 265 of the CRMAs can be ranked as $DM < WM < REM < W-EM = AREM < D-EM$.

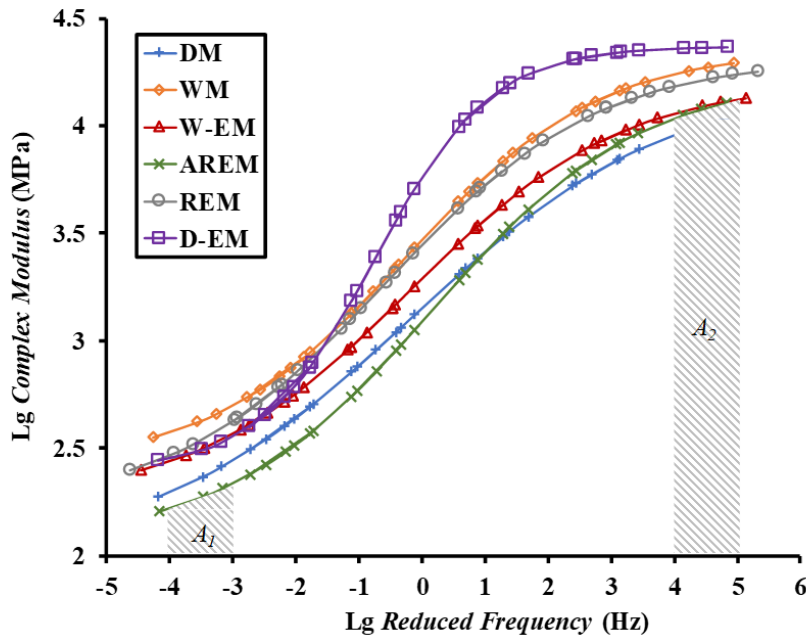


266
 267 **Figure 5. Load cycles of asphalt mixtures**

268 **4.3. Dynamic modulus**

269 A strain range, within which asphalt mixture behaves as a linear visco-elastic material, is defined
 270 as the linear visco-elastic (LVE) region. Previous research documented that the dynamic modulus
 271 (ratio of stress to strain) of asphalt mixture within the LVE region has a good correlation with the
 272 service performance of asphalt mixture (Yu et al., 2019a). Generally, asphalt mixture with higher
 273 modulus at high service temperature (or low loading frequency) shows superior rutting resistance.
 274 Asphalt mixture with lower modulus at low service temperature (or high loading frequency)

275 appears to be less susceptible to cracking. To investigate the overall performance of asphalt mixture
 276 within a wide frequency range, master curves of dynamic modulus at a reference temperature of
 277 20 °C was established based on the dynamic modulus at different temperatures through the time-
 278 temperature superposition principle. Figure 6 illustrates the master curves of dynamic modulus of
 279 all asphalt mixtures.



280
 281 **Figure 6. Master curves of dynamic modulus test results**

282 As expected, the complex modules of asphalt mixtures are different at all frequencies
 283 revealing the effect of mixing process on overall rheological property of asphalt mixture. It can be
 284 observed that there is a significant difference between D-EM and other asphalt mixtures in terms
 285 of complex modulus at almost all frequencies. Among the other asphalt mixtures, the master curves
 286 of DM and AREM are nearly coincide indicating their similar rheological behavior. Similarly, it
 287 can be concluded that the performance of WM is comparable to that of REM. Moreover, it can be
 288 found that DM may present the best low-temperature performance, as it showed the lowest modulus
 289 at high frequencies. WM may present the best high-temperature performance because its dynamic
 290 modulus at low frequencies was the highest.

291 The area enclosed by the master curve and reduced frequency reveals the performance of
 292 asphalt mixture within the corresponding frequency range. For instance, area, A_1 , enclosed by low-
 293 frequency (1E-4 Hz to 1E-3 Hz) and AREM's master curve indicates the high-temperature
 294 performance of AREM. Similarly, A_2 shows AREM's low-temperature performance. A
 295 dimensionless indicator S was used to quantify the overall rheological performance of asphalt
 296 mixture in this study. S is defined by Equation 3. Asphalt mixture with higher S presents a better
 297 overall rheological performance.

$$S = \frac{A_1}{A_2} \quad \text{Equation 3}$$

298 A_1 , A_2 and S of asphalt mixtures are listed in Table 4. Darker color indicates better performance.
 299 Same as Figure 6, WM and DM had the best high-temperature and low-temperature performance,
 300 respectively. Based on S , it was found that WM performed the best overall performance followed
 301 by W-EM, and REM. The overall performance of AREM was the poorest one.

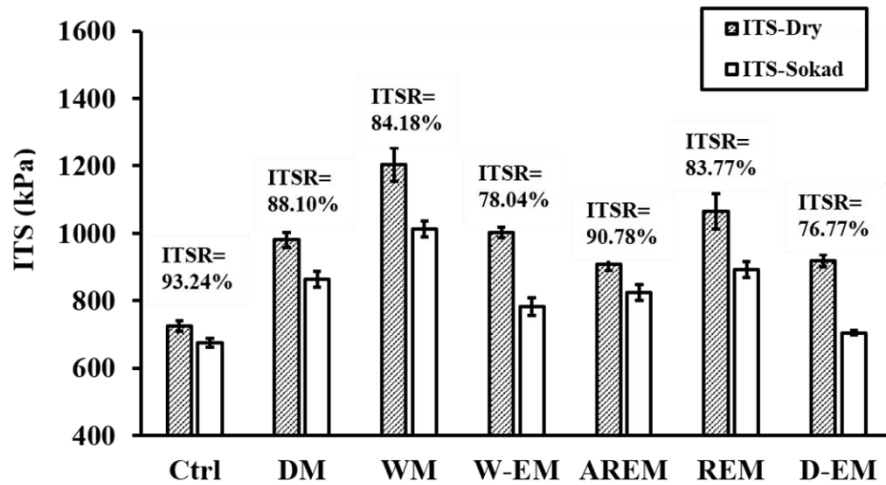
302 **Table 4. Overall rheological performance of asphalt mixtures**

Asphalt mixture	A1	A2	S
DM	2.364	4.006	0.590
WM	2.631	4.268	0.616
W-EM	2.495	4.095	0.609
AREM	2.269	4.08	0.556
REM	2.539	4.171	0.609
D-EM	2.492	4.363	0.571

303

304 **4.4. Moisture damage resistance**

305 Moisture damage is one of the main distresses which significantly decreases the service life of
306 asphalt pavement. Moisture penetrates into the asphalt mixture through cracks and connected pores.
307 As a consequence of freezing, these penetrated moistures swell and deforms the asphalt mixture
308 leading to crack propagation and an increase in the connected pores. This process deteriorates the
309 mechanical properties of asphalt mixture. ITSR reflects the moisture damage resistance of asphalt
310 mixture. Higher ITSR refers to superior moisture damage resistance. Figure 7 presents the ITS of
311 asphalt mixture before and after freeze-thaw cycle as well as the corresponding ITSR.



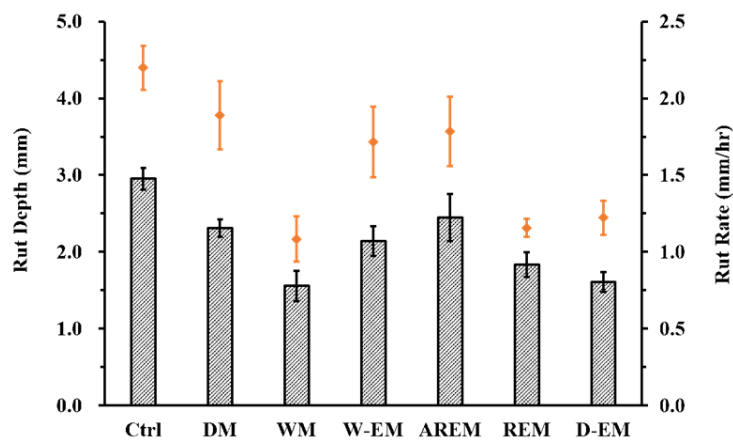
312
313 **Figure 7. ITS of asphalt mixtures before and after freeze-thaw cycle**

314 As can be observed, regardless of the moisture condition of asphalt mixture, ITS of CRMAs
315 were higher than that of Ctrl. This is because of the stiffness enhancing effect of CRM. The ITS
316 changed with the changing of the mixing procedure indicating the non-negligible influence of
317 mixing procedure on stiffness of asphalt mixture. Although the ITSR values of all the asphalt
318 mixtures ranged from around 77% to 93%, which were much higher than the minimum threshold
319 value (70 % to 80 %), the ISTR values of CRMAs were lower than that of Ctrl. By comparing the
320 ITSR values among all the CRMAs, it was found that mixing procedure affected the moisture

321 damage resistance of asphalt mixture. AREM and D-EM exhibited the highest and the lowest ITSR
 322 value, respectively. This finding could be explained by the variation of adhesive effect between
 323 asphalt binder and aggregate because moisture is easier to penetrate to asphalt mixture with worse
 324 bonding effect. Therefore, asphalt mixture with worse bonding effect may shows lower ISTR value.
 325 The ranking of CMRAs prepared with different mixing processes with respect to moisture damage
 326 resistance performance from low to high was D-EM, W-EM, REM, WM, DM and AREM.

327 **4.5. Rutting resistance**

328 Rutting occurs on the wheel path of pavement. It attributes to the cumulative permanent
 329 deformation of pavement resulting from repeated wheel loads at high temperature. Rutting mainly
 330 happens in summer when the capacity of asphalt mixture is lower and is more sensitive to wheel
 331 load. Therefore, rutting resistance is an important indicator to evaluate the high-temperature of
 332 asphalt mixture. Higher rut depth reveals poorer rutting resistance. Figure 8 presents the results of
 333 the WLT test.



334

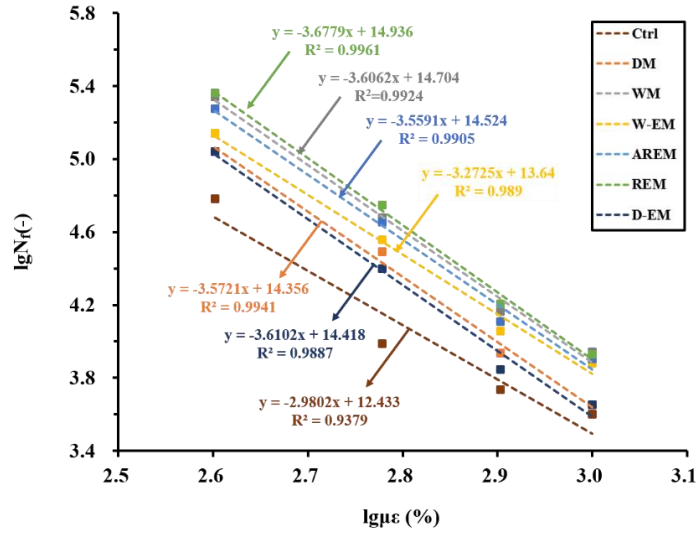
335

Figure 8. Rut depth and rut rate of asphalt mixtures

336 Based on the rut depth and rut rate, it can be found that adding CRM helps to improve the
337 rutting resistance of asphalt mixture. Based on the measured rut depth, the rutting resistance of
338 asphalt mixtures, from low to high, can be ranked as Ctrl, AREM, DM, W-EM, REM, D-EM, WM.
339 Based on the rut rate, the ranking was Ctrl, DM, AREM, W-EM, D-EM, REM, WM. Again, this
340 finding demonstrated the effect of mixing process on the service performance of CRMAs.

341 **4.6. Fatigue performance**

342 During the service life of asphalt pavement, fatigue cracking is a primary mode of failure that
343 is caused by undergoing millions of repeated load applications. Fatigue cracking occurs if the
344 applied loads exceed the designed capacity of fatigue resistance of the asphalt mixture. These
345 cracks will quickly extend to a much larger area. Fatigue cracking brings considerable cost in
346 maintenance and rehabilitation, reduce the ride quality (due to the increased roughness of pavement
347 surface) and significantly decrease the pavement's service life. Therefore, it is of fundamental to
348 assess the fatigue performance of asphalt mixtures. Figure 9 presents the measured fatigue life of
349 asphalt mixtures at different strain levels. Obviously, the fatigue life of all the asphalt mixtures
350 decrease as the increase of strain amplitude. The fatigue line of REM, WM, AREM were in a
351 similar region indicating the corresponding CRMAs exhibited similar fatigue performance under
352 strain loadings.



353

354

Figure 9. N_f vs. strain of asphalt mixtures

355 The classical fatigue relationship model described in Monismith et al. (1961) is reproduced in

356 Equation 4.

$$N_f = a \left(\frac{1}{\varepsilon} \right)^b \quad \text{Equation 4}$$

357 where, a and b are material specific constants, which are considered to be related to the fatigue

358 property of asphalt mixture, determined by recession analysis. ε is strain level.

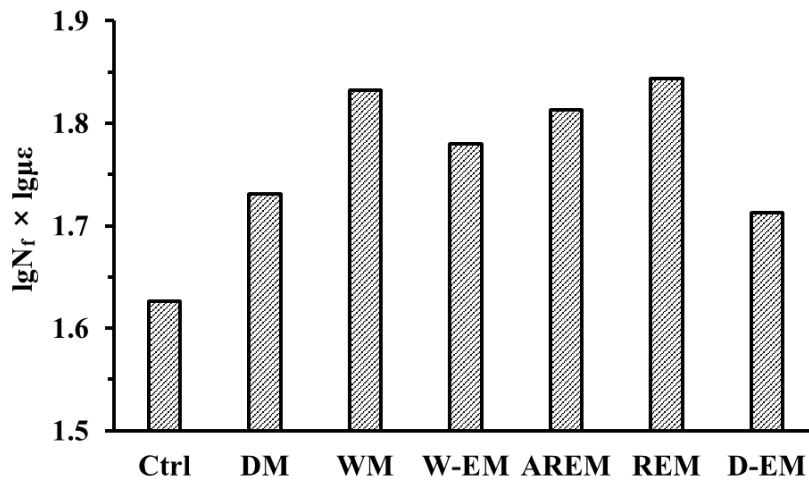
359 Constant a and b of different asphalt mixtures are listed in Table 5.

360

Table 5. Values of a and b of different asphalt mixtures

Asphalt mixture	a	b
Ctrl	6.89E-10	4.10E+00
DM	6.75E-07	3.30E+00
WM	2.97E-08	3.79E+00
W-EM	4.98E-07	3.37E+00
AREM	1.11E-07	3.60E+00
REM	1.59E-07	3.58E+00

361 The area enclosed by the N_f -strain curve and $lg\mu\epsilon$, as shown in Figure 10, was used as an
 362 indicator to quantify the differences between the asphalt mixtures with respect to the entire fatigue
 363 performance. The larger the area, the better the fatigue resistance. As can be seen, the fatigue
 364 resistance of Ctrl is much poorer than that of CRMAs, which proved the positive effect of CRM
 365 on fatigue resistance of asphalt mixture. Among all the CRMAs, fatigue resistance of DM and D-
 366 EM were poorer than that of the rest CRMAs.

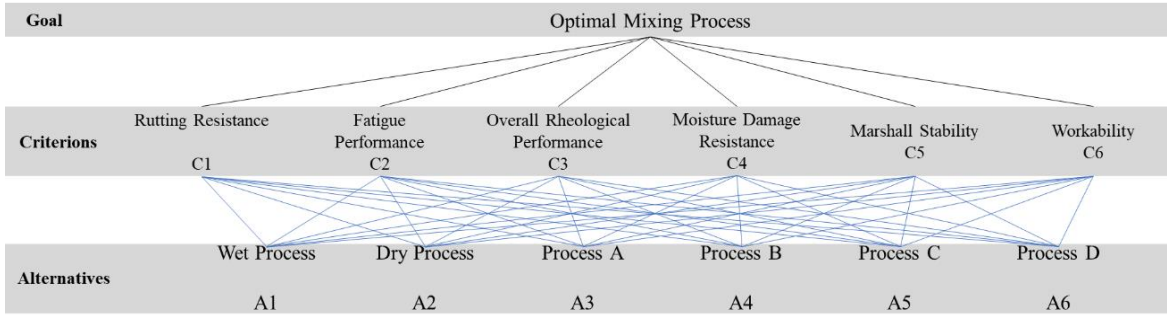


367

368 **Figure 10. Fatigue performance of asphalt mixtures**

369 **4.7. Analytic Hierarchy Process**

370 AHP was used in this study to determine the optimal mixing procedure of CRMA considering the
 371 overall service performance. As shown in Figure 11, optimal mixing procedure was set as goal (G),
 372 six performance related indicators, including rutting resistance (C1), fatigue performance (C2),
 373 overall rheological performance (C3), moisture damage resistance (C4), Marshall stability (C5),
 374 and workability (C6) were set as criteria (C), mixing procedures were set as alternatives (A).



375

376

Figure 11. Diagram of hierarchy

377

378

379

380

381

382

In southern China, rutting performance is the most critical indicator in terms of pavement designing and construction followed by fatigue performance and overall rheological behavior. Therefore, the ranking of the six performance related indicators with respect to importance is rutting performance > fatigue performance = overall rheological performance > moisture damage resistance > Marshall stability > workability. Thus, the corresponding pairwise comparison matrix can be obtained as shown below:

383

$$G = \begin{bmatrix} 1 & 2 & 2 & 3 & 7 & 9 \\ 1/2 & 1 & 1 & 2 & 6 & 7 \\ 1/2 & 1 & 1 & 2 & 6 & 7 \\ 1/3 & 1/2 & 1/2 & 1 & 3 & 5 \\ 1/7 & 1/6 & 1/6 & 1/3 & 1 & 3 \\ 1/9 & 1/7 & 1/7 & 1/5 & 1/3 & 1 \end{bmatrix}$$

384

385

The principle eigenvalue of matrix G (λ_G) and the corresponding eigenvector (X_G) were then calculated:

386

$$\lambda_G = 6.1296$$

387

$$X_G = [0.7262, 0.4465, 0.4465, 0.2470, 0.0984, 0.0566]^T$$

388

After normalization, X_G can be rewritten as follows:

389

$$\omega_G = [0.3593, 0.2209, 0.2209, 0.1222, 0.0487, 0.0280]^T$$

390 Since the consistency ratio of matrix G was 0.021, verified the consistency of pairwise
 391 comparison matrix, the priorities of six performance-related indicators is 0.3593, 0.2209, 0.2209,
 392 0.1222, 0.0487, 0.0280, respectively.

393 Pairwise comparisons were then performed on the alternatives, namely, A_1 to A_6 , for
 394 determining their priorities to six indicators based on the experimental results. The matrixes of
 395 pairwise comparison of the alternatives are given below according to the quantified differences in
 396 terms of importance to six indicators.

$$397 \quad C_1 = \begin{bmatrix} 1 & 4 & 2 & 9 & 2 & 1 \\ 1/4 & 1 & 1/2 & 2 & 1/3 & 1/4 \\ 1/2 & 2 & 1 & 4 & 1/2 & 1/2 \\ 1/9 & 1/2 & 1/4 & 1 & 1/7 & 1/9 \\ 1/2 & 3 & 2 & 7 & 1 & 1 \\ 1 & 4 & 2 & 9 & 1 & 1 \end{bmatrix} \quad C_2 = \begin{bmatrix} 1 & 4 & 2 & 1 & 1 & 8 \\ 1/4 & 1 & 1/2 & 1/3 & 1/4 & 2 \\ 1/2 & 2 & 1 & 1/2 & 1/2 & 5 \\ 1 & 3 & 2 & 1 & 1 & 7 \\ 1 & 4 & 2 & 1 & 1 & 9 \\ 1/8 & 1/2 & 1/5 & 1/7 & 1/9 & 1 \end{bmatrix}$$

$$398 \quad C_3 = \begin{bmatrix} 1 & 2 & 1 & 9 & 1 & 3 \\ 1/2 & 1 & 1 & 6 & 1 & 2 \\ 1 & 1 & 1 & 8 & 1 & 3 \\ 1/9 & 1/6 & 1/8 & 1 & 1/8 & 1/3 \\ 1 & 1 & 1 & 8 & 1 & 3 \\ 1/3 & 1/2 & 1/3 & 3 & 1/3 & 1 \end{bmatrix} \quad C_4 = \begin{bmatrix} 1 & 1 & 3 & 1/2 & 1 & 5 \\ 1 & 1 & 4 & 1 & 2 & 8 \\ 1/3 & 1/4 & 1 & 1/5 & 1/3 & 2 \\ 2 & 1 & 5 & 1 & 2 & 9 \\ 1 & 1/2 & 3 & 1/2 & 1 & 5 \\ 1/5 & 1/8 & 1/2 & 1/9 & 1/5 & 1 \end{bmatrix}$$

$$399 \quad C_5 = \begin{bmatrix} 1 & 2 & 3 & 9 & 2 & 1 \\ 1/2 & 1 & 2 & 6 & 1 & 1 \\ 1/3 & 1/2 & 1 & 4 & 1 & 1/2 \\ 1/9 & 1/6 & 1/4 & 1 & 1/4 & 1/7 \\ 1/2 & 1 & 1 & 4 & 1 & 1/2 \\ 1 & 1 & 2 & 7 & 2 & 1 \end{bmatrix} \quad C_6 = \begin{bmatrix} 1 & 5 & 1/2 & 1/2 & 1 & 1/2 \\ 1/5 & 1 & 1/8 & 1/8 & 1/5 & 1/9 \\ 2 & 8 & 1 & 1 & 1 & 1 \\ 2 & 8 & 1 & 1 & 1 & 1 \\ 1 & 5 & 1 & 1 & 1 & 1/2 \\ 2 & 9 & 1 & 1 & 2 & 1 \end{bmatrix}$$

400 The principle eigenvalues (λ) of pairwise comparison matrixes and the corresponding C.R.
 401 are listed in Table 6.

402

403

Table 6. Principle eigenvalues and C.R. of pairwise comparison matrixes

	C1	C2	C3	C4	C5	C6
λ	6.046	6.017	6.047	6.048	6.067	6.071
C.R.	0.007	0.003	0.007	0.008	0.011	0.011

404 As can be seen, the C.R. of all the pairwise comparison matrixes are smaller than 0.1 revealing
 405 the consistency of the matrixes. The corresponding priority eigenvectors, ω_{Ci} , of six alternatives
 406 can be calculated:

$$407 \quad \omega_{C1} = [0.2969, 0.0670, 0.1281, 0.0314, 0.2153, 0.2613]^T$$

$$408 \quad \omega_{C2} = [0.2590, 0.0681, 0.1347, 0.2425, 0.2642, 0.0314]^T$$

$$409 \quad \omega_{C3} = [0.2595, 0.1807, 0.2250, 0.0282, 0.2250, 0.0815]^T$$

$$410 \quad \omega_{C4} = [0.1817, 0.2597, 0.0605, 0.3051, 0.1603, 0.0327]^T$$

$$411 \quad \omega_{C5} = [0.2967, 0.1850, 0.1130, 0.0316, 0.1364, 0.2372]^T$$

$$412 \quad \omega_{C6} = [0.1266, 0.0276, 0.2174, 0.2174, 0.1624, 0.2487]^T$$

413 The priorities of alternatives, namely, mixing sequence, to the overall service performance of
 414 asphalt mixture was calculated in accordance with Figure 11. The calculated priorities with respect
 415 to the overall performance of asphalt mixture were presented in Figure 12. Asphalt mixture
 416 prepared by mixing procedure with higher priority shows better overall service performance.

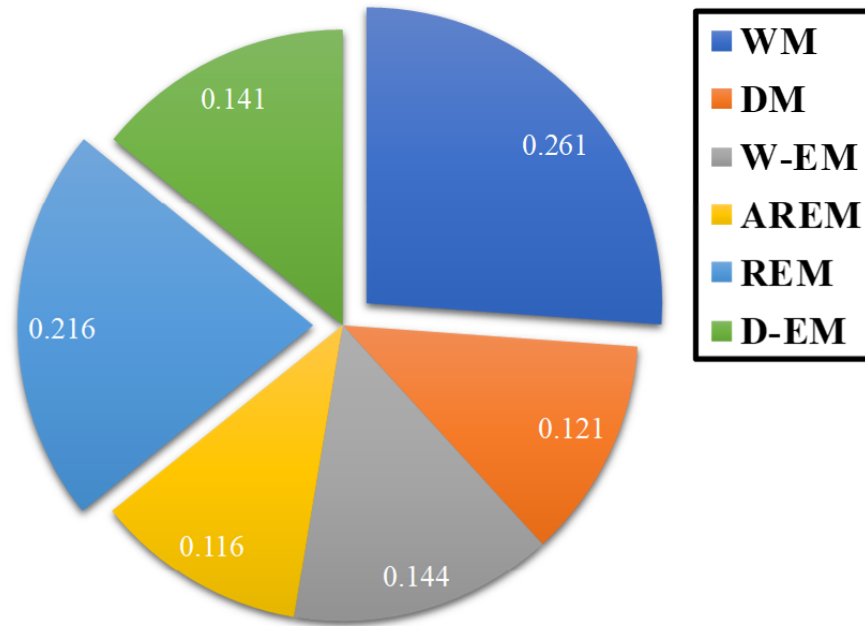


Figure 12. Priorities of mixing procedure

417

418

419 The data presented in this figure indicates that the conventional wet mix CRMA shown the
 420 top priority followed by REM, while AREM had the lowest priority. Among all the WCRMAs,
 421 REM had the first priority revealing the best overall service performance. In addition, the priority
 422 of W-EM was similar to that of D-EM revealing the similar overall service performances.

423 **5. SUMMARY AND FINDINGS**

424 In this study, the differences among the engineering performance including workability, high-
 425 temperature performance, moisture damage resistance and fatigue performance of CRMAs
 426 resulting from varied mixing sequences were investigated through laboratory experiments. Based
 427 on the experimental results, the differences of CRMAs in terms of engineering performance were
 428 quantified. The optimal mixing procedure of CRMA in terms of best overall engineering
 429 performance was determined by means of AHP. The following summarizes the major findings of
 430 this study:

- 431 • Crumb rubber enhances the high-temperature and fatigue performance of asphalt mixture.
432 However, it has opposite effect on the moisture damage resistance of asphalt mixture.
- 433 • The incorporation of surfactant additive, Evotherm-DAT, slightly compromises the
434 engineering performance of CRMA.
- 435 • For the warm rubberized asphalt mixtures, the effect of the mixing sequence on their
436 engineering performance is significant.
- 437 • The optimal preparing sequence to produce warm rubberized asphalt is to make rubber
438 absorb the liquid surfactant first, then incorporating the modified rubber to raw asphalt and
439 finally blending the warm asphalt rubber binder to aggregates.

440 Finally, this study proves that the effect of mixing sequence on engineering performance of
441 warm rubberized asphalt mixture is significant. However, it is worth noting that this study focuses
442 on samples with liquid surfactant additive. The effects of mixing sequence on rubberized mixtures
443 with other types of WMA additives like FT-wax and zeolite will be investigated in future studies.

444 **ACKNOWLEDGEMENT**

445 The authors acknowledged the financial support from National Natural Science Foundation of China
446 (51808228), Fundamental Research Funds for the Central Universities (2018MS92), German
447 Research Foundation (OE 514/10-1) and China Postdoctoral Science Foundation funded project
448 (2018M643089). Trademark or manufacturers' names appear in this paper only because they are
449 considered essential to the object of this paper.

450 **REFERENCE**

451 Ahmadinia, E., Zargar, M., Karim, M.R., Abdelaziz, M., & Shafigh, P., 2011. Using waste
452 plastic bottles as additive for stone mastic asphalt. *Materials & Design*. 32 (10), 4844-4849.

453 American Association of State and Highway Transportation Officials, 2017. AASHTO R
454 83 Standard practice for preparation of cylindrical performance test specimens using the Superpave
455 Gyratory Compactor (SGC).

456 American Association of State and Highway Transportation Officials, 2011. AASHTO
457 T342, Standard method of test for determining dynamic modulus of hot mix asphalt (HMA).

458 ASTM International, 2015. ASTM D6372, Standard practice for design, testing, and
459 construction of microsurfacing.

460 ASTM International, 2015. ASTM D6927, Standard test method for Marshall stability and
461 flow of asphalt mixtures.

462 ASTM International, 2017. ASTM D6931, Standard test method for indirect tensile (IDT)
463 strength of asphalt mixtures.

464 ASTM International, 2010. ASTM D7460, Standard test method for determining fatigue
465 failure of compacted asphalt concrete subjected to repeated flexural bending.

466 Bai, F., Yang, X., & Zeng, G., 2016. A stochastic viscoelastic–viscoplastic constitutive
467 model and its application to crumb rubber modified asphalt mixtures. *Materials & Design*. 89, 802-
468 809.

469 Cao, W., & Liu, S., 2012. Performance evaluation of asphalt-rubber stone matrix asphalt
470 mixtures with warm mix asphalt additives. *Journal of Testing and Evaluation*. 41 (1), 141-147.

471 Chávez, F., Marcobal, J., & Gallego, J., 2019. Laboratory evaluation of the mechanical
472 properties of asphalt mixtures with rubber incorporated by the wet, dry, and semi-wet process.
473 *Construction and Building Materials*. 205, 164-174.

474 Ding, X., Ma, T., Zhang, W., & Zhang, D., 2017. Experimental study of stable crumb rubber
475 asphalt and asphalt mixture. *Construction and Building Materials*. 157, 975-981.

476 Fontes, L. P. T. L., Trichês, G., Pais, J. C., & Pereira, P. A. A., 2010. Evaluating permanent
477 deformation in asphalt rubber mixtures. *Construction and Building Materials*. 24 (7), 1193-1200.

478 Gong, H., Huang, B., & Shu, X., 2018. Field performance evaluation of asphalt mixtures
479 containing high percentage of RAP using LTPP data. *Construction and Building Materials*. 176,
480 118-128.

481 Huang, B., Mohammad, L. N., Graves, P. S., & Abadie, C., 2002. Louisiana experience
482 with crumb rubber-modified hot-mix asphalt pavement. *Transportation Research Record*. 1789 (1),
483 1-13.

484 Jia, X., Ye, F., & Huang, B., 2015. Utilization of Construction and Demolition Wastes in
485 Low-Volume Roads for Rural Areas in China. *Transportation Research Record*. 2474 (1), 39-47.

486 Leng, Z., Zhang, Z., Zhang, Y., Wang, Y., Yu, H., & Ling, T., 2018. Laboratory evaluation
487 of electromagnetic density gauges for hot-mix asphalt mixture density measurement. *Construction*
488 *and Building Materials*. 158, 1055-1064.

489 Ling, T., Lu, Y., Zhang, Z., Li, C., & Oeser, M., 2019. Value-added application of waste
490 rubber and waste plastic in asphalt binder as a multifunctional additive. *Materials*. 12 (8), 1280.

491 Liu, Y., Han, S., Zhang, Z., & Xu, O., 2012. Design and evaluation of gap-graded asphalt
492 rubber mixtures. *Materials & Design*. 35, 873-877.

493 Mohajerani, A., Tanriverdi, Y., Nguyen, B. T., Wong, K. K., Dissanayake, H. N., Johnson,
494 L., Whitfield, D., Thomson, G., & Rezaei, A., 2017. Physico-mechanical properties of asphalt
495 concrete incorporated with encapsulated cigarette butts. *Construction and Building Materials*. 153,
496 69-80.

497 Monismith, C. L., Secor, K. E., & Blackmer, W., 1961. Asphalt mixture behavior in
498 repeated flexure. *Proceedings, Association of Asphalt Paving Technologists*. 30, 188 -222.

499 Moreno, F., Sol, M., Martín, J., Pérez, M., & Rubio, M. C., 2013. The effect of crumb
500 rubber modifier on the resistance of asphalt mixes to plastic deformation. *Materials & Design*. 47,
501 274-280.

502 Oliveira, J. R. M., Silva, H. M. R. D., Abreu, L. P. F., & Fernandes, S. R. M., 2013. Use of
503 a warm mix asphalt additive to reduce the production temperatures and to improve the performance
504 of asphalt rubber mixtures. *Journal of Cleaner Production*. 41, 15-22.

505 Paje, S. E., Bueno, M., Teran, F., Miro, R., Perez-Jimenez, F., & Martínez, A. H., 2010.
506 Acoustic field evaluation of asphalt mixtures with crumb rubber. *Applied Acoustics*. 71, 578-82.

507 Ranieri, M., Costa, L., Olivera, J. R. M., Silva, H. M. R. D., & Celauro, C., 2017. Asphalt
508 surface mixtures with improved performance using waste polymers via dry and wet processes.
509 *Journal of Materials in Civil Engineering*. 29 (10), 04017169.

510 Rubio, M. C., Martínez, G., Baena, L., & Moreno, F., 2012. Warm mix asphalt: An
511 overview. *Journal of Cleaner Production*. 24, 76-84.

512 Ruiz, G., Chávez, F., Santamaría, S., Araujo, W., Timaná, J., & Schmitt, R., 2018.
513 Laboratory evaluation of seashells used as fine aggregate in hot mix asphalt. *International Journal*
514 *of Pavement Engineering*. 1-9.

515 Saaty, T. L., 1990. How to make a decision: the analytic hierarchy process. *European*
516 *Journal of Operational Research*. 48 (1), 9-26.

517 Song, W., Huang, B., & Shu, X., 2018. Influence of warm-mix asphalt technology and
518 rejuvenator on performance of asphalt mixtures containing 50% reclaimed asphalt pavement.
519 *Journal of Cleaner Production*. 192, 191-198.

520 Vázquez, V. F., Luong, J., Bueno, M., Terán, F., & Paje, S. E., 2016. Assessment of an
521 action against environmental noise: Acoustic durability of a pavement surface with crumb rubber.
522 Science of Total Environment. 542, 223-230.

523 Wang, H., Dang, Z., You, Z., & Cao, D., 2012. Effect of warm mixture asphalt (WMA)
524 additives on high failure temperature properties for crumb rubber modified (CRM) binders.
525 Construction and Building Materials. 35, 281-288.

526 Wei, H., He, Q., Jiao, Y., Chen, J., & Hu, M., 2016. Evaluation of anti-icing performance
527 for crumb rubber and diatomite compound modified asphalt mixture. Construction and Building
528 Materials. 107, 109-116.

529 Xiao, F., Zhao, W., & Amirkhanian, S. N., 2010. Laboratory investigation of fatigue
530 characteristics of rubberized asphalt mixtures containing warm asphalt additives at a low
531 temperature. Journal of Testing and Evaluation. 39 (2), 290-295.

532 Xiao, F., Punith, V., & Amirkhanian, S. N., 2012. Effects of non-foaming WMA additives
533 on asphalt binders at high performance temperatures. Fuel. 94, 144-155.

534 Xu, H., Xing, C., Zhang, H., Li, H., & Tan, Y., 2019. Moisture seepage in asphalt mixture
535 using X-ray imaging technology. International Journal of Heat and Mass Transfer. 131, 375-384.

536 Yu, H., Leng, Z., Zhou, Z., Shih, K., Xiao, F., & Gao, Z., 2017. Optimization of preparation
537 procedure of liquid warm mix additive modified asphalt rubber. Journal of Cleaner Production.
538 141, 336-345.

539 Yu, H., Leng, Z., Dong, Z., Tan, Z., Guo, F., & Yan, J., 2018. Workability and mechanical
540 property characterization of asphalt rubber mixtures modified with various warm mix asphalt
541 additives. Construction and Building Materials. 175, 392-401.

542 Yu, H., Zhu, Z., Zhang, Z., Yu, J., Oeser, M., & Wang, D., 2019a. Recycling waste
543 packaging tape into bituminous mixtures towards enhanced mechanical properties and
544 environmental benefits. *Journal of Cleaner Production*. 229, 22-31.

545 Yu, H., Zhu, Z., & Wang, D., 2019b. Evaluation and validation of fatigue testing methods
546 for rubberized bituminous specimens. *Transportation Research Record*. 0361198119841308.

547 Zaumanis, M., Poulikakos, L. D., & Partl, M. N., 2018. Performance-based design of
548 asphalt mixtures and review of key parameters. *Materials & Design*. 141, 185-201.

549 Zhao, S., Huang, B., Shu, X., Jia, X., & Woods, M., 2012. Laboratory Performance
550 Evaluation of Warm-Mix Asphalt Containing High Percentages of Reclaimed Asphalt Pavement.
551 *Transportation Research Record*. 2294(1), 98-105.

552 Zhao, S., Huang, B., Shu, X., & Woods, M., 2013. Comparative evaluation of warm mix
553 asphalt containing high percentages of reclaimed asphalt pavement. *Construction and Building*
554 *Materials*. 44, 92-100.

555

556

557

558

559

560

561

562

563

564

565

566

567

568 **FIGURE CAPTIONS**

- 569 1. Aggregate gradation.
- 570 2. Experimental tests conducted in this study.
- 571 3. Main scales for pairwise comparison.
- 572 4. Marshall stability and flow values of asphalt mixtures.
- 573 5. Load cycles of asphalt mixtures.
- 574 6. Master curves of dynamic modulus test results.
- 575 7. ITS of asphalt mixtures before and after freeze-thaw cycle.
- 576 8. Rut depth and rut rate of asphalt mixtures.
- 577 9. N_f vs. strain of asphalt mixtures.
- 578 10. Fatigue performance of asphalt mixtures.
- 579 11. Diagram of hierarchy.
- 580 12. Priorities of mixing procedure.

581

582

583

584

585

586

587

588 **TABLE CAPTIONS**

- 589 1. Engineering properties of virgin binder.
- 590 2. Gradation of crumb rubber.
- 591 3. Involved mixing processes.
- 592 4. Overall rheological performance of asphalt mixtures.
- 593 5. Values of a and b of different asphalt mixtures.
- 594 6. Principle eigenvalues and C.R. of pairwise comparison matrixes.